Microwave-Assisted Biosynthesis of Ag/ZrO2 Catalyst with Excellent Activity toward Selective Oxidation of 1,2-Propanediol

Feng Yang,[†] Xiaolian Jing,[‡] Jiale Huang,*[,‡] Daohua Sun,[‡] and Qingbiao Li*[,†,‡,§]

[†]Environmental Science Research Center, College of the Environment & Ecology and [‡]Department of Chemical and Biochemical Engineering, College of Chemistry and Chemical Engineering, Xiamen University, Xiamen 361005, People's Republic of China
[§]College of Chemistry & Life Science, Quanzhou Normal University, Quanzhou, 362000, People's Republic of China

S *Supporting Information*

ABSTRACT: In the biorefining process, polyols are important intermediates, and the oxidation of polyols toward other value added products is of great significance. This work describes a green and facile biosynthesis method for the preparation of Ag/ZrO2 catalyst for selective oxidation of 1,2-propanediol (a typical polyol). *Cinnamomum comphora* (CC) leaf extract was employed as the reducing and capping agent for the preparation of Ag nanoparticles (NPs) with the assistance of microwave irradiation. The main reducing agents were identified as polyphenols by Fourier transform infrared spectroscopic analysis of CC extracts before and after reaction. After electrostatic adsorption, the NPs were anchored onto the support ZrO2. The Ag/ZrO2 catalysts were found with good dispersity and showed excellent activity toward selective oxidation of 1,2-propanediol. The effects of the preparation conditions on catalyst activity were studied; the optimal condition was obtained (microwave time of 4 min, CC concentration of 12 g/L and Ag loading of 5%). Since the natural capping agents are easy to remove, the catalysts need no calcination treatment before catalytic reaction. Thus, the microwave-assisted biosynthesis appears to be environmentally benign as neither expensive chemicals nor intensive energy consumption is engaged.

1. INTRODUCTION

Methylglyoxal (pyruvaldehyde) is a key intermediate chemical with unique reaction character due to its adjacent carbonyl groups. It has wide applications in the fields of pharmacy, biochemistry, pesticides, and textiles. It is accredited by the U.S. Food and Drug Administration (FDA; No. 121.1164) and the Flavor and Extract Manufacturers Association of the United States (FEMA; No. 2969) for its usage as a spice in foods[1] and the food industry.[2] As a raw material, it can be used for the production of cimetidine (pharmaceutical intermediate), lactic acid, pyruvic acid, cosmetics, and desensitizers. Methylglyoxal can be produced from acetone, glycerol,[3] and 1,2-propanediol.[4] For the acetone route, the flammable, toxic property of acetone and the involvement of the toxic solvent acetonitrile are both potential hazards and have thus limited its industrial production. Direct dehydrogenation of glycerol to methylglyoxal with low yield was found unable to meet the manufacture demand.[3] Therefore, 1,2-propanediol as a mild and cheap chemical was selected as the raw material for the industrial production of methylglyoxal. By this way, a yield of ca. 60% can be achieved through gas phase oxidation with the proper catalyst.[5]

Ag catalyst is the most extensively studied catalyst for the selective oxidation of 1,2-propanediol as Ag is quite effective to provide surface adsorbed oxygen species that are critical to the polyol oxidation.[6] Incipient wetness impregnation is a routine method for the preparation of supported Ag catalyst.[7] In this way, the precursors were adsorbed onto the support and converted into Ag or silver oxide particles by calcination. However, by this means the size of formed particles is uneven and the dispersity of nanoparticlse (NPs) over the support is poor.[8] Therefore, other ways with the aim of controlling the particle size were developed. Generally, two major ways were mostly employed: first, using appropriate reductive and protective agents to synthesize uniform Ag NPs (kinetic and/or thermodynamic control);[9,10] second, trapping Ag precursors inside templates or supports with ordered porous structure so that the Ag NPs could be restricted to small and uniform size.[11−13] However, both methods involved surfactants or expensive templates which need to be removed later by calcination at high temperature (over 500 °C) and that is energy-wasting. Bioreduction reveals its advantages at these aspects. First, in the synthesis procedure, NPs with uniform size can be prepared using extract of natural materials (the alternates of chemicals or surfactants).[14,15] Second, in the loading procedure, biomolecules were reported to be effective in improving the dispersity of NPs over the support and preventing the NPs from aggregation during sintering.[16−19] In addition, most of the biomolecules are easily removed by calcination at a much lower temperature than that for the surfactants or templates. Therefore, neither expensive chemicals nor great energy consumption is involved in the bioreduction method.

In recent years, microwave irradiation has been frequently used for the preparation of nanomaterials due to its rapid and even heating from molecular friction.[20,21] Bhat et al.[22] have synthesized Ag NPs using areca nut with microwave heating. In this work, microwave radiation was employed to promote bioreduction to provide a higher reduction rate. A higher

reduction rate favors the formation of polycrystalline structures which are more active in the catalytic reactions.[23] With homogeneous nucleation at a higher reaction rate, NPs with small size can be formed.[24] Moreover, the reduction time could be shortened from hours to minutes. Hence, bioreduction using *Cinnamomum camphora* with the assistance of microwave irradiation was designed for the green and facile preparation of Ag/ZrO_2 catalyst. Also, the effects of preparation conditions on catalyst activity were studied. The prepared catalyst with reduced amount (200 mg) finally gave a high yield of methylglyoxal. Besides, the calcination of the catalyst was omitted as the biomasses were easily removed under the reaction temperature of 340 °C.

2. EXPERIMENTAL SECTION

2.1. Chemicals. *C. camphora* (CC) leaves, provided by XiaMen Peony Fragrance & Chemicals Co. Ltd., were first thoroughly washed with deionized (DI) water and naturally air-dried. Then the leaves were crushed into fine powders by a high speed pulverizer for later use. The support ZrO_2 was purchased from Xiamen Luyin Reagent Glass Instrument Co. Ltd., and it was calcined at 500 °C for 2 h to remove impurities before use. Other chemicals were purchased from Sinopharm Chemical Reagent Co. Ltd. and used as received.

2.2. Catalyst Synthesis. CC extract was prepared by a water-extraction process: typically, 5 g of CC leaf powders was dispersed in 100 mL of deionized water with magnetic stirring in a oil bath at 30 °C for 12 h. After that, the suspension was filtrated and the obtained filter liquor was defined as 50 $g \cdot L^{-1}$ CC extract. The catalyst was prepared by a microwave-assisted biosynthesis method. First, Ag colloids were synthesized as follows: a certain volume of CC extract was mixed with 1000 μL of $AgNO_3$ (100 mM) and the total volume was set to 30 mL by the addition of deionized water. Then the solution was exposed to microwave irradiation at a power of 110 W for several minutes; generally, the color of the solution turned from pale yellow to dark red as a result of the formation of Ag NPs. The obtained NPs were immobilized onto the ZrO_2 support through electrostatic attraction: the ZrO_2 powders were dispersed in the as-prepared colloid and then the pH value of the suspension was adjusted to 2.5 by HNO_3 (the surface charges of Ag NPs and the support were in inverse states). After stirring for 2 h at ambient temperature, the slurry was filtrated and the resulting solid was dried at 50 °C for 4 h as the catalyst.

2.3. Characterization. The UV−vis adsorption spectra of the Ag colloids were recorded on a Thermal Evolution 200 spectrometer; all samples were diluted 15 times with DI water before measurement. The Fourier transform infrared (FT-IR) spectra of CC extract after reaction was recorded on an Nicolet 6700 FTIR spectrometer (Thermo Fisher), generated Ag NPs were removed by centrifugation at 12 000 rpm for 15 min, and the supernatant was vacuum freeze-dried at −50 °C for analysis. Transmission electron microscopy (TEM) images of the samples were captured on a Tecnai F30 microscope. The size of the Ag NPs was estimated via statistical analysis of the TEM micrographs with SigmaScan Pro software (SPSS Inc., version 4.01.003). Powder X-ray diffraction (XRD) experiment was conducted over a Rigaku Ultima IV X-ray diffractometer using Cu $K\alpha$ radiation, operating at 40 kV and 30 mA. The thermogravimetric (TG) analysis was performed on an SDT Q600 thermogravimetric analyzer with a heating rate of 10 °C· min^{-1} under flowing air (100 $mL \cdot min^{-1}$). X-ray photoelectron

spectroscopy (XPS) was performed using a PHI Quantum-2000 spectrometer equipped with a hemispherical electron analyzer and an Al $K\alpha$ (1486.6 eV) X-ray source, and C 1s was used as a reference to calibrate the obtained data.

2.4. Catalytic Activity Test. The catalytic reaction was carried out in a homemade atmospheric microscale fixed bed reactor, in which a 45 cm glass tube with 1.2 cm i.d. was used. The reaction temperature was controlled by a tube furnace equipped with a thermoelectric couple. A micropump (Beijing Xingda, SZB-2) was used for the feeding of 1,2-propanediol. Air was used as the oxidant with a gas velocity of 140 $mL \cdot min^{-1}$. After condensation of the effluent with icy water, the product was collected and analyzed on a gas chromatograph equipped with a SE-30 capillary column and a flame ionization detector (ShangHai Huaai GC-9560; injection chamber temperature 260 °C, column temperature 100 °C); the calculation was based on the peak area by the external standard method and three parallel samples were captured at each temperature point.

3. RESULTS AND DISCUSSION

3.1. Characterization. *3.1.1. UV−Vis and FT-IR Analysis.* UV−vis spectra of Ag colloids prepared with different exposure times to microwave irradiation are shown in Figure 1. The
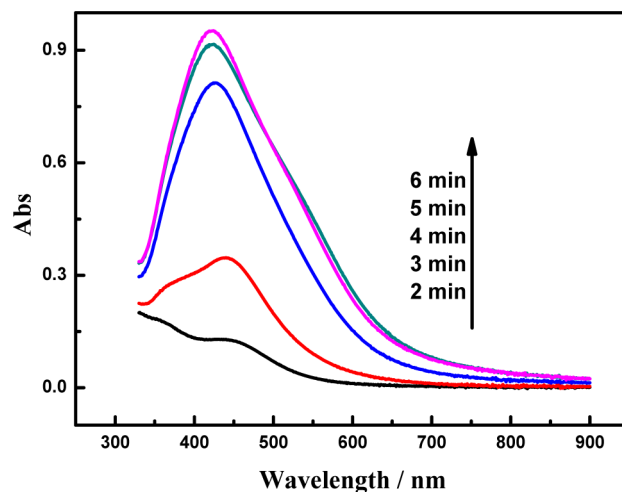

Figure 1. UV−vis spectra of Ag colloid prepared with different microwave times.

adsorption peaks at 423 nm were ascribed to the surface plasmon resonance (SPR) peak of silver,[25] indicating the formation of Ag NPs after bioreduction. The reaction balance was achieved at 5 min as the stopping of the peak growth was observed. In addition, the concentration of Ag^+ ions was measured by atomic absorption spectroscopy (AAS) so that a conversion of 93.74% for Ag^+ at this point was calculated (Supporting Information, Figure S1; the actual conversion was considered very close or equal to 100% as there still were small NPs that cannot be completely separated before measurement). The rapid growth of the peak before 5 min indicated the high reduction rate of Ag^+. Since the size of the NPs increased with extending reaction time and noticing that small NPs are more active for the reaction,[26] it is deduced that irradiation time of ca. 4 min was appropriate for the adequate reduction of Ag^+ while keeping the formed NPs small. No chemicals were engaged in the preparation of Ag NPs owing to the abundant reductive and protective agents in CC extract.

The CC extracts after reaction with different volumes of $AgNO_3$ were characterized by FT-IR spectroscopy to identify the reducing agents for $AgNO_3$. The spectra are displayed in Figure 2. The peaks at 1762 and 1711 cm^{-1} were assigned to
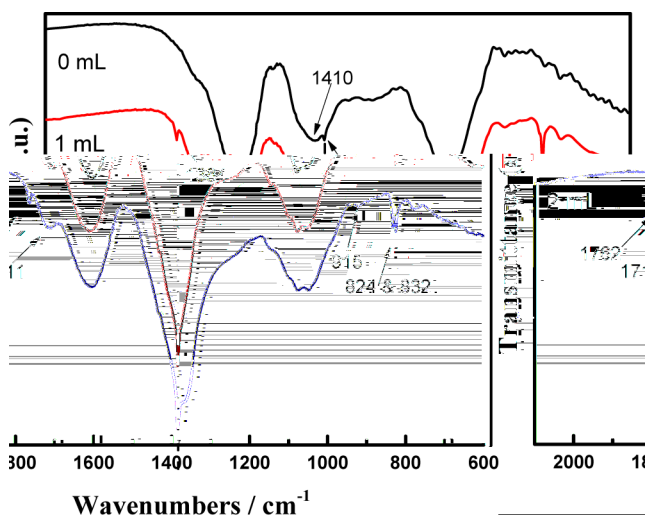

Figure 2. FT-IR spectra of CC extract after reaction with different dosages of $AgNO_3$.

carbonyl stretching and were traceable to the formation of a phenoxide structure.[27] The peak at 1410 cm^{-1} corresponded to the combined vibration of O−H deformation and C−O stretching in phenols; it disappeared after reaction with $AgNO_3$ which suggested the consumption of phenols in the redox reaction. The enhancement of the peak at 1384 cm^{-1} was a result of aldehyde groups increased from oxidation of hydroxyl groups. It was found that a peak at 824 cm^{-1} appeared after reaction and a concomitant split peak showed up at 832

cm^{-1} with more $AgNO_3$ added; the two peaks were assigned to the out-of-plane deformation vibration of C−H bonds of mono- and disubstituted benzoquinones, respectively. As an additional feature, the weak peak at 915 cm^{-1} also implied the presence of benzoquinones. Therefore, the reducing abilities of CC extract could be attributed to polyphenols. The phenolic hydroxyl group was most likely the electron-donating group as its oxidative product benzoquinone was found after the redox reaction.

3.1.2. Transmission Electron Microscopy (TEM) Analysis. TEM was used to determine the morphology and size information on Ag NPs and Ag/ZrO_2 catalyst. Images of Ag colloids prepared with different microwave irradiation times are shown in Figure 3. As can be seen, Ag NPs of spheres or quasi-spheres with size around 20 nm were synthesized after microwave irradiation. The particle sizes were in direct proportion to the microwave time as longer irradiation time led to generation of more Ag atoms which were then absorbed by NPs for their growth. The particle size increased quickly in the initial 4 min as a result of the rapid reduction, and then (5−6 min) the growth of the particles became slow as the Ag precursors were almost consumed. Meanwhile, the frequency variation in the histogram of the NPs demonstrated that aggregation between particles took place, leading to the decrease of small NPs and the increase of large ones.

The Ag/ZrO_2 catalyst with 5 wt % Ag loading (microwave irradiation time 4 min) was also captured by TEM, and the images of the catalyst before and after reaction are shown in Figure 4. It can be seen that, after the electrostatic adsorption, Ag NPs were successfully anchored onto the support with good dispersity. It is worth noting that the biosynthesized Ag NPs were modified by biomolecules with carbonyl groups which were reported to be beneficial to enhance the immobilization and improve the dispersity of NPs over the support by means of adsorption and bridging.[16,28] The particle size remained
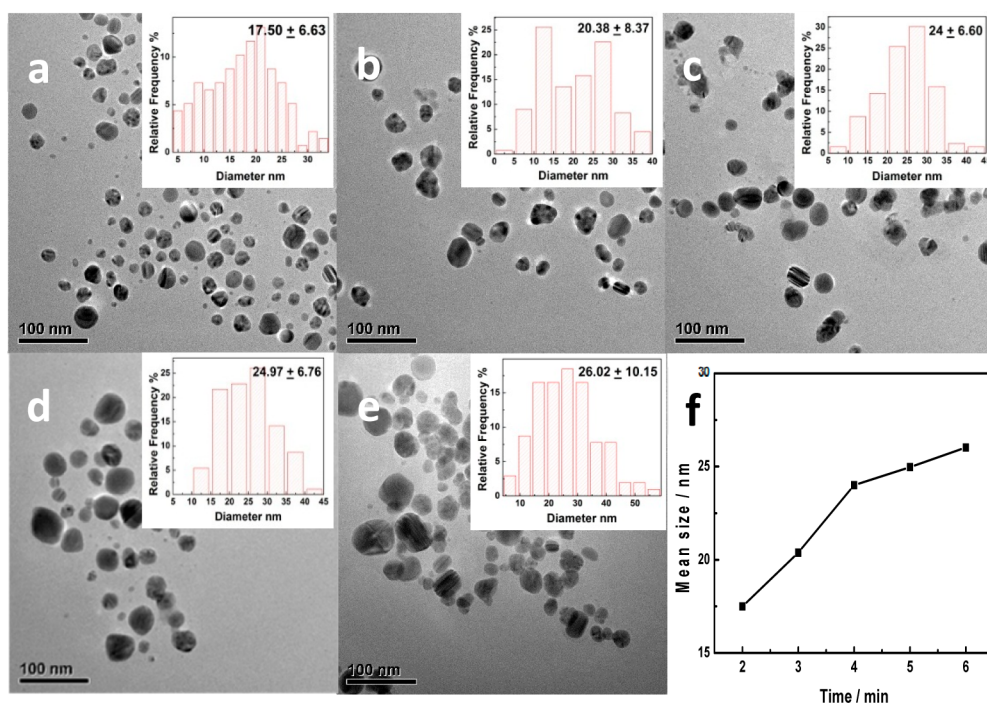

Figure 3. TEM images of Ag colloids prepared with different microwave times: (a) 2, (b) 3, (c) 4, (d) 5, and (e) 6 min. (f) Their mean size versus irradiation time.
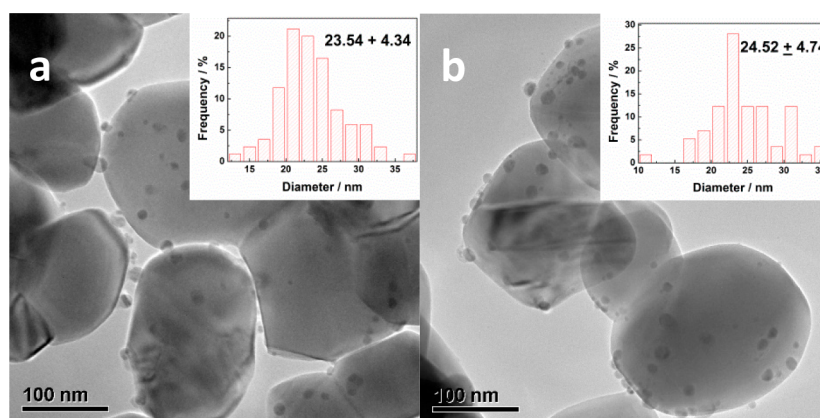
Figure 4. TEM images of Ag/ZrO$_2$ catalyst (a) before and (b) after reaction. Conditions: 5% Ag loading, 12 g·L^{-1} CC, irradiation time 4 min.
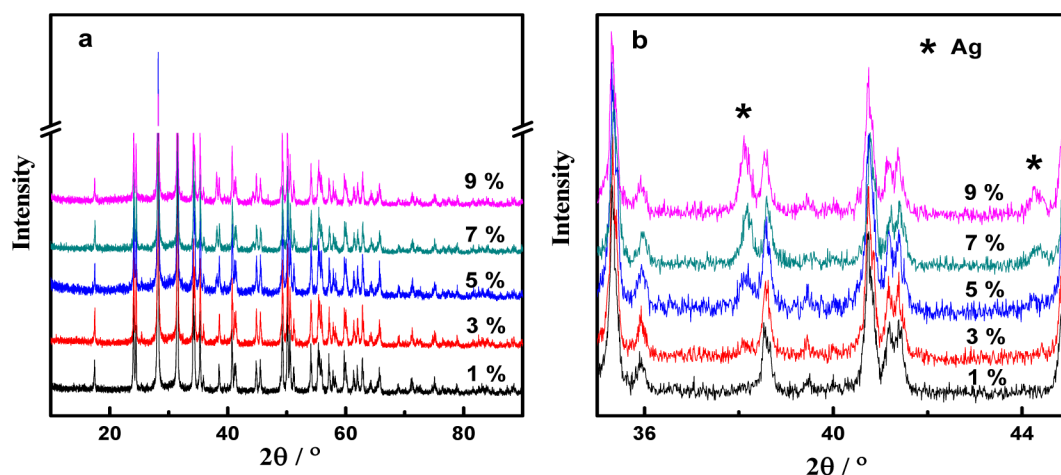

Figure 5. XRD patterns of Ag/ZrO$_2$ catalysts with different Ag loadings: (a) overall profiles and (b) magnification of Ag peaks.

unchanged after the catalytic reaction. These results suggested that the microwave-assisted biosynthesis method was effective for the preparation of supported Ag/ZrO$_2$ catalyst.

3.1.3. XRD and TG Analysis. The crystalline structure of the catalysts was characterized by powder X-ray diffraction (XRD). The XRD patterns of catalysts with different Ag loadings are displayed in Figure 5. Diffraction peaks corresponding to ZrO$_2$ of monoclinic phase at 17, 24, 28, and 31° were observed (Figure 5a).[29] The support was in single monoclinic phase as no diffraction peaks for tetragonal or cubic phase were found. The peaks at 38.1 and 44.1° were ascribed to the (111) and (200) facets of face-centered-cubic Ag (Figure 5b).[30] The peak intensities increased with higher Ag loadings, confirming the good incorporation of Ag NPs and the ZrO$_2$ support. The broad half-peak width of the peak indicated the tiny crystal size of the Ag NPs. No silver oxide species were formed according to the XRD results as only diffraction peaks of metallic Ag appeared.

Thermogravimetric experiment was performed to investigate the decomposition behavior of the biomolecules adsorbed on the catalyst. The obtained TG/differential thermogravimetric (DTG) curves of the as-prepared catalyst are shown in Figure 6. Since the support was calcined at 500 °C beforehand, the weight loss from the support below 500 °C can be ignored. The TG curve of the fresh catalyst showed a sharp decrease at 250−340 °C, which was assigned to the decomposition of the biomolecules. The peak in the DTG curve also illustrated that
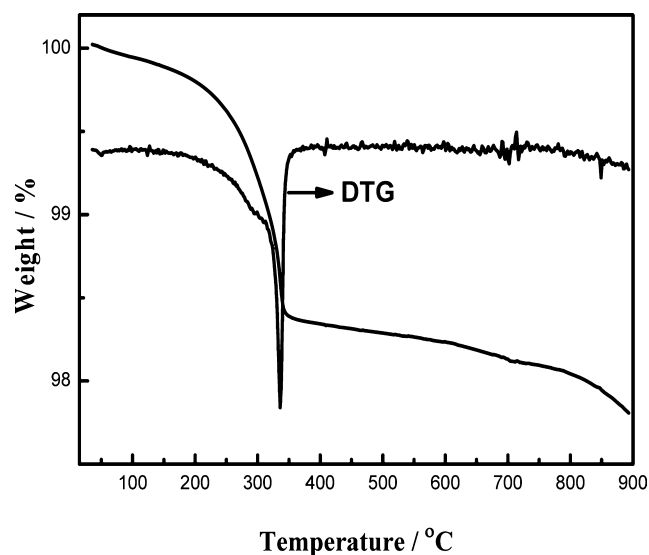

Figure 6. TG/DTG curve of fresh catalyst. Conditions: 5% Ag loading, 12 g·L^{-1} CC, irradiation time 4 min.

most of the biomolecules were combusted at the 340 °C region. The slight weight loss over 340 °C was from the further combustion of the residual biomasses. The total weight loss was about 2.2 wt %, and biomolecules accounted for a high proportion. TG experiment demonstrated that the biosynthe-
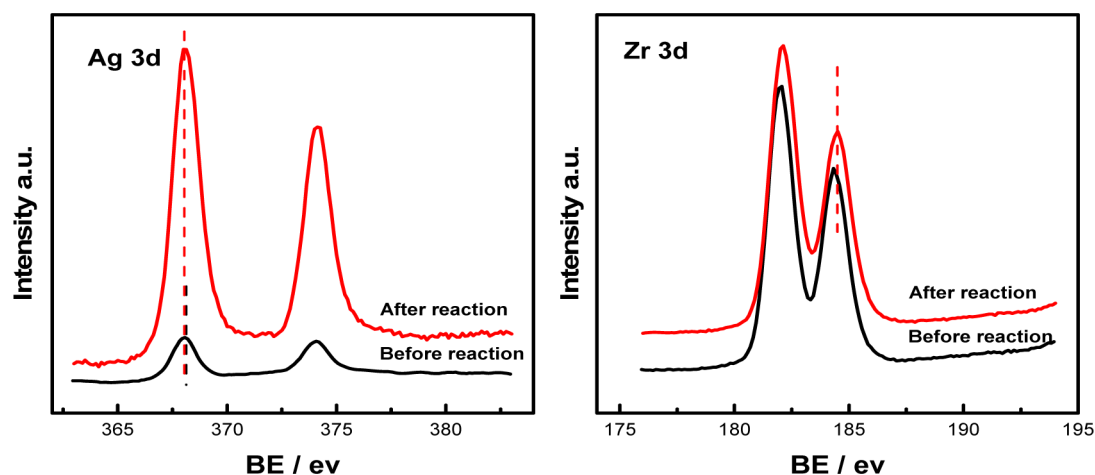
Figure 7. XPS spectra of Ag 3d and Zr 3d regions for Ag/ZrO$_2$ before and after reaction. Conditions: 5% Ag loading, 12 g·L^{-1} CC, irradiation time 4 min.

sized Ag catalyst contained some biomolecules from CC extract, most of which would be decomposed at 340 °C.

3.1.4. XPS Analysis. XPS spectra of Ag 3d and Zr 3d regions for the catalyst before and after reaction are shown in Figure 7. The fresh catalyst showed two peaks located at 368.0 and 374.0 eV, which were associated with metallic Ag.[31] The two peaks validated the successful reduction of Ag precursors and also the immobilization of Ag NPs upon the support. After reaction the peak intensity for Ag was greatly enhanced, which indicated the removal of surface-adsorbed biomolecules as well as the revealing of Ag NPs. In addition, slight binding energy (BE) shifts of Ag and Zr after reaction were observed, which was a result from electron transfer between the metal and the support. The shift to lower BE value for Ag and to higher BE value for Zr indicated that the electron transfer was from Ag to Zr^{4+}.[32] The main change in the catalyst after the catalytic reaction was resulted from the combustion of the biomolecules at 340 °C, which also can be seen in the TG curve (Figure 6). The change of the interaction between the metal and the support was, however, very slight in view of the tiny BE shifts.

3.2. Catalyst Activity. *3.2.1. Effect of Reaction Temperature.* The effect of reaction temperature on the catalytic reaction was studied, and the result is given in Figure 8. The conversion of 1,2-propanediol increased with higher reaction
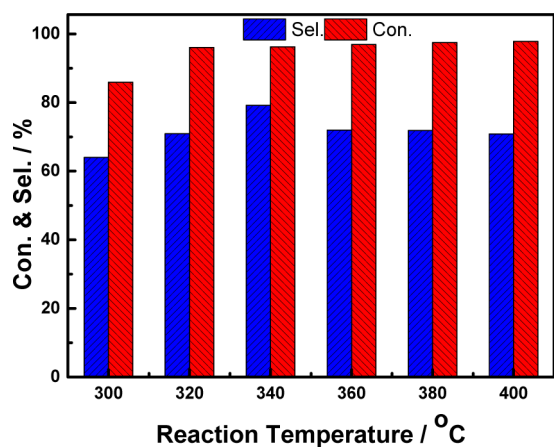
temperature, as higher temperature is beneficial for the activation of the O−H bond and the scission of the C−H bond in 1,2-propanediol. When the temperature was elevated to 340 °C, the conversion reached the maximum of 96% and remained constant regardless of higher temperatures. But the selectivity of methylglyoxal decreased with further elevation of the temperature. This was due to the aggravation of C−C scission of methylglyoxal at higher temperatures (>340 °C), leading to additional production of byproducts (aldehyde and carbon dioxide) and continuous decrease in the selectivity of methylglyoxal. Therefore, the reaction temperature of 340 °C with the highest yield of methylglyoxal was selected for later assessments.

3.2.2. Effect of Microwave Radiation Time. The influence of microwave time on catalyst activity was investigated. The conversion and selectivity first increased with extending irradiation time (Figure 9a). When irradiation time was prolonged over 4 min, the conversion became close to 100% and did not increase anymore but the selectivity began to decrease. This can be explained by the curve in Figure 9b (the absorbance of the Ag colloids at 423 nm as a function of irradiation time). The absorbance which is positively related to the Ag NP concentration increased quickly in the initial 4 min. As a result, the catalyst activity increased over time within 4 min as more NPs formed. After 4 min the absorbance hardly increased as it was already close to the maximum. However, the aggregation of NPs occurred with increasing irradiation time at higher temperature as can be seen in TEM results. As a matter of course the selectivity of the catalyst decreased. Considering influences from both aspects (NP concentration and NP size), 4 min was proven to be the optimal irradiation time.

3.2.3. Effect of CC Extract Concentration. The effect of CC extract concentration on catalyst activity was investigated. As shown in Figure 10, the highest yield of methylglyoxal was obtained with the catalyst prepared using 12 g·L^{-1} CC extract. When lower concentration of CC extract was used, Ag precursors could not be fully reduced. As a result, the active sites in the catalyst (the amount of produced Ag NPs) were insufficient for the reaction and the catalyst activity dropped. On the contrary, when denser CC extract was used, excess biomasses were adsorbed onto the catalyst. The excessive biomasses tended to block the active sites by adsorbing over Ag NPs (depicted in XPS result); by this way, they became
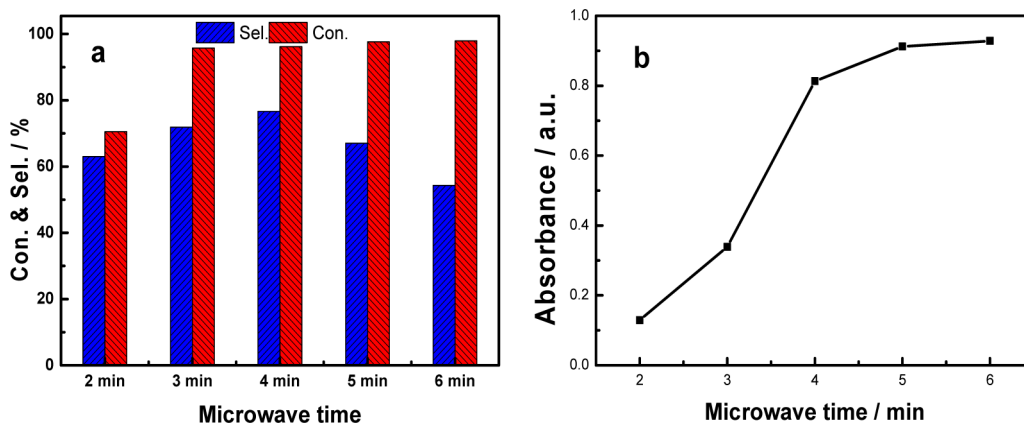

Figure 8. Effect of reaction temperature on catalyst activity. Conditions: 5% Ag loading, 12 g·L^{-1} CC, irradiation time 4 min.

Figure 9. Effect of microwave irradiation time on catalyst activity: (a) catalyst activity versus irradiation time; (b) absorbance of Ag colloids at 423 nm versus irradiation time. Conditions: 5% Ag loading, 12 g·L^{-1} CC, reaction temperature 340 °C.
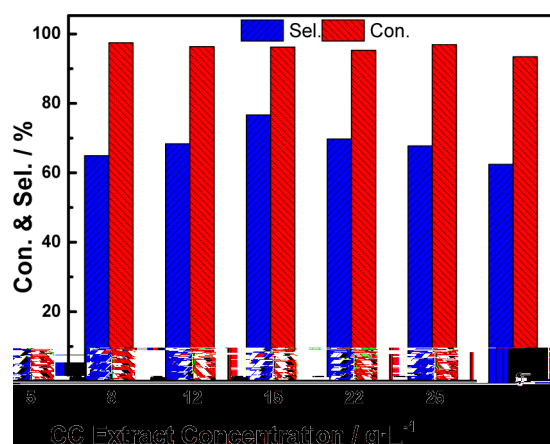

Figure 10. Effect of CC extract concentration on catalyst performance. Conditions: 5% Ag loading, irradiation time 4 min, reaction temperature 340 °C.
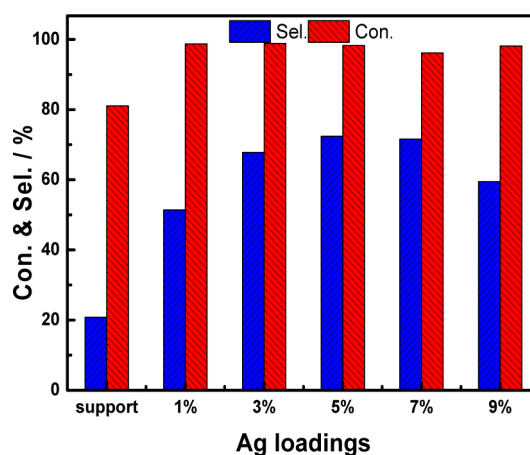

Figure 11. Effect of Ag loading on catalyst activity. Conditions: 12 g·L^{-1} CC, irradiation time 4 min, reaction temperature 340 °C.

detrimental to the catalyst activity. Finally, the proper concentration of CC extract was determined to be 12 g·L^{-1}.

3.2.4. Effect of Ag Loading. The effect of Ag loading on the catalyst activity was investigated. First, all Ag colloids were prepared with a fixed AgNO$_3$/CC ratio to exclude the size difference of the NPs. Different Ag loadings were achieved by varying the dosage of the support in the loading step. The catalytic performances of the catalysts are shown in Figure 11. A control sample of the pure support was also tested. The results showed that the selectivity to methylglyoxal was very low and many unidentified byproducts were produced. The selectivity was doubled if 1% Ag was loaded onto the support, and the multifarious byproducts almost disappeared except for hydroxyacetone. The 5 wt % Ag/ZrO$_2$ catalyst possessed the highest yield of methylglyoxal. As analyzed in TG experiments, with the immobilization of Ag NPs, biomasses were simultaneously introduced onto the catalyst. Though most of the biomasses were combusted during the assessment, there still existed residues from incomplete combustion or ingredients tolerant to the reaction temperature. Also, the residues (carbon species) accumulated will ultimately decrease the catalyst activity by blocking the active sites.

To compare with the oil-bath way, a control sample was prepared by oil-bath heating under the obtained optimal conditions. The results (Supporting Information, Figures S2−S4) showed that the formed NPs were larger and the selectivity

of the catalyst was much lower when employing an oil bath; besides, the reaction time was extended to hours to achieve the overall reduction[25] other than several minutes when using microwave irradiation.

3.3. Catalyst Durability. Catalyst durability is an important performance index in industrial application. Hence, the stability of the as-prepared catalyst was assessed. As shown in Figure 12,
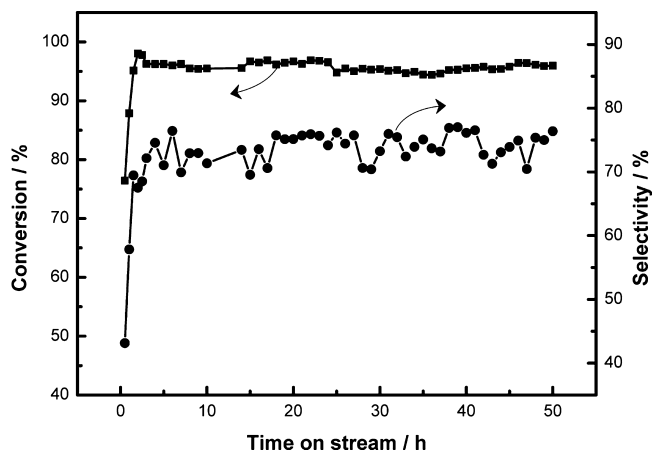

Figure 12. Catalyst durability. Conditions: 5% Ag loading, 12 g·L^{-1} CC, irradiation time 4 min, reaction temperature 340 °C.

the gradual increase of conversion and selectivity at the initial time indicated the gradual decomposition of biomasses. As stated in section 3.1.3, that excess biomass would block the active sites and decrease the catalyst activity, therefore with biomass decomposing at the early time the concurrent enhancement of catalyst activity was observed. Since the residual biomolecules adsorbed over NPs were conductive to preventing the NPs from aggregation and to promoting the desorption of product molecules,[17,26] remarkable stability of the as-prepared catalyst was obtained. As can be seen in Figure 12, no obvious decrease in conversion or selectivity was observed within 50 h of assessment. The XRD pattern for the catalyst after reaction remained the same as before (Supporting Information, Figure S5), which indicated the excellent stability of the catalyst.

4. CONCLUSIONS

Herein, a facile and green biosynthesis method for preparation of supported Ag/ZrO_2 catalyst was proposed. All preparation processes were carried out at mild conditions, and the as-prepared catalyst does not need calcination before use. Due to the small and uniform size of the Ag NPs and the good dispersity of the NPs over the support, the catalyst exhibited excellent activity toward selective oxidation of 1,2-propanediol. Conversion of 97% and selectivity of 79% to methylglyoxal were obtained at the reaction temperature of 340 °C with the catalyst of 5% Ag loading. It was speculated from FTIR analysis that polyphenols were the main reducing components, and the abundant natural capping agents played a vital role in controlling the NP size and improving the dispersity of NPs over the support. TG results showed that most of the biomasses from bioreduction were combusted at 340 °C and that is why the catalysts need no calcination before testing. But when too much biomass is introduced, the succeeding accumulation of carbon species from incomplete burning will also decrease the catalyst activity. Last, from all the results above, we believe this method has great potential for the green preparation of highly active catalysts in other catalytic reactions.

■ ASSOCIATED CONTENT

Ⓢ Supporting Information

AAS standard curve and reduction degree of Ag versus microwave time (Figure S1), contrast of UV−vis spectra of Ag colloids prepared by oil-bath and microwave heating (Figure S2), TEM images of the NPs and catalyst prepared by oil-bath heating (Figure S3), catalytic activity contrast of the catalysts prepared by the two methods (Figure S4), XRD profile of the catalyst after reaction (Figure S5), and XRD pattern of Ag NPs before loading (Figure S6). The Supporting Information is available free of charge on the ACS Publications website at DOI: 10.1021/ie5047363.

■ AUTHOR INFORMATION

Corresponding Authors

*E-mail: cola@xmu.edu.cn (J.H.).
*E-mail: kelqb@xmu.edu.cn. Tel.: (+86) 592-2189595. Fax: (+86) 592-2184822 (Q.L.).

Notes

The authors declare no competing financial interest.

■ REFERENCES

(1) Rosing, E. A.; Turksma, H. Process for the preparation of a savory flavor. U.S. Patent US 6,074,683 A, 2000.
(2) Hofmann, T.; Schieberle, P. 2-Oxopropanal, hydroxy-2-propanone, and 1-pyrroline important intermediates in the generation of the roast-smelling food flavor compounds 2-acetyl-1-pyrroline and 2-acetyltetrahydropyridine. *J. Agric. Food Chem.* **1998**, *46*, 2270−2277.
(3) Baltes, H.; Leupold, E. I. 2-Oxopropanal (Methylglyoxal) by Oxidation of Glycerin in the Gas Phase. *Angew. Chem., Int. Ed.* **1982**, *21*, 540−540.
(4) Baltes, H.; Leupold, E. I.Methyl glyoxal by oxidation of 1,2-propylenediol in a gas phase on a heterogeneous catalyst. U.S. Patent US 4,355,187, 2003.
(5) Shen, J.; Du, J.-M.; Huang, J.-J.; Yang, X.-Y.; Shen, W.; Xu, H.-L.; Fan, K.-N. Gas-phase Selective Oxidation of 1,2-Propylene Glycol over Ag/ZrO2 Catalyst. *Acta Chim. Sin.* **2007**, *65*, 403−408.
(6) Ayre, C. R.; Madix, R. J. The adsorption and reaction of 1,2-propanediol on Ag(110) under oxygen lean conditions. *Surf. Sci.* **1994**, *303*, 279−296.
(7) Bamwenda, G. R.; Tsubota, S.; Nakamura, T.; Haruta, M. The influence of the preparation methods on the catalytic activity of platinum and gold supported on TiO2 for CO oxidation. *Catal. Lett.* **1997**, *44*, 83−87.
(8) Huang, Z. W.; Cui, F.; Kang, H. X.; Chen, J.; Zhang, X. Z.; Xia, C. G. Highly dispersed silica-supported copper nanoparticles prepared by precipitation-gel method: A simple but efficient and stable catalyst for glycerol hydrogenolysis. *Chem. Mater.* **2008**, *20*, 5090−5099.
(9) Raji, V.; Chakraborty, M.; Parikh, P. A. Catalytic Performance of Silica-Supported Silver Nanoparticles for Liquid-Phase Oxidation of Ethylbenzene. *Ind. Eng. Chem. Res.* **2012**, *51*, 5691−5698.
(10) Li, J.; Zhu, J.; Liu, X. Ultrafine silver nanoparticles obtained from ethylene glycol at room temperature: catalyzed by tungstate ions. *Dalton Trans.* **2014**, *43*, 132−137.
(11) Tian, D.; Yong, G. P.; Dai, Y.; Yan, X. Y.; Liu, S. M. CO Oxidation Catalyzed by Ag/SBA-15 Catalysts Prepared via in situ Reduction: The Influence of Reducing Agents. *Catal. Lett.* **2009**, *130*, 211−216.
(12) Ma, L.; Jia, L. H.; Guo, X. F.; Xiang, L. J. Catalytic activity of Ag/SBA-15 for low-temperature gas-phase selective oxidation of benzyl alcohol to benzaldehyde. *Chin. J. Catal.* **2014**, *35*, 108−119.
(13) Eddahbi, A.; Ider, M.; Tabti, M.; Ouaskit, S.; Moussetade, M.; Abderrafi, K. A novel synthetic route for preparation of Ag nanoparticles in aqueous emulsion of copolymer template. *J. Optoelectron. Adv. Mater.* **2013**, *15*, 1228−1232.
(14) Iravani, S. Green synthesis of metal nanoparticles using plants. *Green Chem.* **2011**, *13*, 2638.
(15) Mittal, A. K.; Chisti, Y.; Banerjee, U. C. Synthesis of metallic nanoparticles using plant extracts. *Biotechnol. Adv.* **2013**, *31*, 346−356.
(16) Sun, D. H.; Wang, H. X.; Zhang, G. L.; Huang, J. L.; Li, Q. B. Preparation of Ag/alpha-Al2O3 for ethylene epoxidation through thermal decomposition assisted by extract of Cinnamomum camphora. *RSC Adv.* **2013**, *3*, 20732−20737.
(17) Du, M. M.; Zhan, G. W.; Yang, X.; Wang, H. X.; Lin, W. S.; Zhou, Y.; Zhu, J.; Lin, L.; Huang, J. L.; Sun, D. H.; Jia, L. S.; Li, Q. B. Ionic liquid-enhanced immobilization of biosynthesized Au nanoparticles on TS-1 toward efficient catalysts for propylene epoxidation. *J. Catal.* **2011**, *283*, 192−201.
(18) Huang, J.; Liu, C.; Sun, D.; Hong, Y.; Du, M.; Odoom-Wubah, T.; Fang, W.; Li, Q. Biosynthesized gold nanoparticles supported over TS-1 toward efficient catalyst for epoxidation of styrene. *Chem. Eng. J.* **2014**, *235*, 215−223.
(19) Hong, Y.; Jing, X.; Huang, J.; Sun, D.; Odoom-Wubah, T.; Yang, F.; Du, M.; Li, Q. Biosynthesized bimetallic Au-Pd nanoparticles

supported on TiO2 for solvent-free oxidation of benzyl alcohol. *ACS Sustainable Chem. Eng.* **2014**, *2*, 1752−1759.

(20) Shojaie, A. F.; Loghmani, M. H. La3+ and Zr4+ co-doped anatase nano TiO2 by sol-microwave method. *Chem. Eng. J.* **2010**, *157*, 263−269.

(21) Choi, A.; Palanisamy, K.; Kim, Y.; Yoon, J.; Park, J. H.; Lee, S. W.; Yoon, W. S.; Kim, K. B. Microwave-assisted hydrothermal synthesis of electrochemically active nano-sized Li2MnO3 dispersed on carbon nanotube network for lithium ion batteries. *J. Alloys Compd.* **2014**, *591*, 356−361.

(22) Bhat, R.; Ganachari, S.; Deshpande, R.; Ravindra, G.; Venkataraman, A. Rapid Biosynthesis of Silver Nanoparticles Using Areca Nut (Areca catechu) Extract Under Microwave-Assistance. *J. Cluster Sci.* **2013**, *24*, 107−114.

(23) Gao, X. P.; Bao, J. L.; Pan, G. L.; Zhu, H. Y.; Huang, P. X.; Wu, F.; Song, D. Y. Preparation and electrochemical performance of polycrystalline and single crystalline CuO nanorods as anode materials for Li ion battery. *J. Phys. Chem. B* **2004**, *108*, 5547−5551.

(24) Zhan, G. W.; Huang, J. L.; Lin, L. Q.; Lin, W. S.; Emmanuel, K.; Li, Q. B. Synthesis of gold nanoparticles by Cacumen Platycladi leaf extract and its simulated solution: toward the plant-mediated biosynthetic mechanism. *J. Nanopart. Res.* **2011**, *13*, 4957−4968.

(25) Huang, J. L.; Zhan, G. W.; Zheng, B. Y.; Sun, D. H.; Lu, F. F.; Lin, Y.; Chen, H. M.; Zheng, Z. D.; Zheng, Y. M.; Li, Q. B. Biogenic Silver Nanoparticles by Cacumen Platycladi Extract: Synthesis, Formation Mechanism, and Antibacterial Activity. *Ind. Eng. Chem. Res. .* **2011**, *50*, 9095−9106.

(26) Zhan, G.; Huang, J.; Du, M.; Sun, D.; Abdul-Rauf, I.; Lin, W.; Hong, Y.; Li, Q. Liquid phase oxidation of benzyl alcohol to benzaldehyde with novel uncalcined bioreduction Au catalysts: High activity and durability. *Chem. Eng. J.* **2012**, *187*, 232−238.

(27) Dubey, S. P.; Lahtinen, M.; Sillanpaa, M. Tansy fruit mediated greener synthesis of silver and gold nanoparticles. *Process Biochem.* **2010**, *45*, 1065−1071.

(28) Wu, W.; Huang, J.; Wu, L.; Sun, D.; Lin, L.; Zhou, Y.; Wang, H.; Li, Q. Two-step size- and shape-separation of biosynthesized gold nanoparticles. *Sep. Purif. Technol.* **2013**, *106*, 117−122.

(29) Chen, L.-J.; Tang, Y.; Cui, L.; Ouyang, C.; Shi, S. Charge transfer and formation of Ce3+ upon adsorption of metal atom M (M = Cu, Ag, Au) on CeO2 (100) surface. *J. Power Sources* **2013**, *234*, 69−81.

(30) Zhang, X.; Qu, Z.; Yu, F.; Wang, Y. Progress in carbon monoxide oxidation over nanosized Ag catalysts. *Chin. J. Catal.* **2013**, *34*, 1277−1290.

(31) Moulder, J. F.; Stickle, W. F.; Sobol, P. E.; Bomben, K. D. *Handbook of X-ray Photoelectron Spectroscopy*; Perkin Elmer: Eden Prairie, MN, 1992; Vol. *40*.

(32) Habibi, M.; Sheibani, R. Preparation and characterization of nanocomposite ZnO−Ag thin film containing nano-sized Ag particles: influence of preheating, annealing temperature and silver content on characteristics. *J. Sol-Gel. Sci. Technol.* **2010**, *54*, 195−202.